JTE HCMUTE
ISSN: 2615-9740

JOURNAL OF TECHNICAL EDUCATION SCIENCE
Ho Chi Minh City University of Technology and Education
Website: https://jte.hcmute.edu.vn/
Email: jte@hcmute.edu.vn

Adhesive Strength of Hexadecane on Different Iron Compounds: an MD Approach

Ta Dinh Hien
Ho Chi Minh City University of Technology and Education (HCMUTE), Vietnam
* Corresponding author. *Email: hientd@hcmute.edu.vn*

ARTICLE INFO

Received: 17/12/2021
Revised: 26/1/2022
Accepted: 06/2/2022
Published: 28/2/2022

KEYWORDS

Molecular dynamics simulation;
Hexadecane;
Adsorption;
Iron oxides;
Iron.

ABSTRACT

The lubricity of alkane is a research target for numerous tribological applications in either industrial area or fundamental scientific studies. In the current work, a comparative investigation using a classical molecular dynamics (MD) method is carried out to investigate the effect of pure iron and its oxide surfaces on structural properties, adsorption ability of hexadecane ($C_{16}H_{34}$). A reliable force field (FF) of condensed-phase optimized molecular potentials for atomistic simulation studies (COMPASS) is employed to describe the intra- and intermolecular interactions for hexadecane and its interaction with iron oxide surfaces, while the interaction between hexadecane and pure iron is derived from an ab initio result. Regarding the surfaces, the pure iron surfaces are considered using embedded-atom method/Finnis-Sinclair potential (EAM/FS), while the iron oxide surfaces are constructed using the traditional Buckingham force field. The results reveal that hexadecane shows preferential adsorption on iron oxide surfaces compared to pure iron.

Doi: https://doi.org/10.54644/jte.68.2022.1095

1. Introduction

Hexadecane has been used widely as a base oil lubricant for several decades. Several experimental investigations have been carried out to investigate the adsorption of linear hydrocarbon on metal and metal oxide surfaces. There were also plenty theoretical studies investigating the structural and dynamic properties of alkanes on the solid surfaces [1] – [3]. In some theoretical works [4] – [7] and experimental studies [8, 9], the authors indicated that the linear hydrocarbon adsorbed molecularly on metal and metal oxide surfaces. Compared with graphitic carbon, hydrocarbon interacted weakly on MgO(100) surface, but the adhesive strength became larger on Pt(111) [1], [9]. Although this kind of hydrocarbon has attracted the great attention from researchers, the insight into its adhesive strength with steel surface is not accomplished yet. Wetterer et al. explained for the linear relationship between the desorption energies and chain length, the authors disclosed that the flat alignment of linear hydrocarbon was the source of similar additive energy for each methyl group [3]. However, this linear relationship was retained for the chain length within five methyl groups, a nonlinear relationship was found for the larger number of carbon atoms [10]. This observation was confirmed by an MD simulation by Li et al. [5] who studied the adsorption of linear alkanes on α-Al_2O_3(0001) surface. For pure transition metal surface, such as Fe, Ni, Pt …, the obtained adhesive strength was much larger for short hydrocarbon. For instances, Anderson et al. found that methane reacted on iron surface with an activation energy of roughly 88 kJ/mol [11] - [14]. The smaller values have been found for other surfaces of Ni and Pt.

This work investigates the adsorption of hexadecane on iron and its oxide surfaces, and analysis the influence of crystalline structure on thin adsorbed film. This article was organised in the following order: (1) the implemented methodology and parameters for current calculation, (2) a parameterization procedure for hexadecane-iron adhesive strength to determine the pairwise interaction between iron and hexadecane atoms, (3) the calculation of surface structure for each type of surface and their adsorption energies with hexadecane.

JTE
HCMUTE
ISSN: 2615-9740

JOURNAL OF TECHNICAL EDUCATION SCIENCE
Ho Chi Minh City University of Technology and Education
Website: https://jte.hcmute.edu.vn/
Email: jte@hcmute.edu.vn

2. Methodology

The investigation into lubricant adhesive strength, and the surface properties of both solid and fluid were implemented using the FORCITE module in the commercial software Material Studio 7.0 (MS 7.0). COMPASS FF was applied for lubricant [15], while Buckingham FF was used to construct the iron oxide surfaces. The embedded-atom method/Finnis-Sinclair potential (EAM/FS) was used to describe pure iron surfaces [16]. The parameters for Buckingham potential, as reported by Guillot *et al.*, are presented in Table 1. This potential reproduced appropriate thermodynamic, structural, and transport properties of FeO and Fe_2O_3 compounds in natural silicate melt at low and high pressures [17], [18]. The interactions between surface atoms with fluid atoms and between different lubricant molecules were determined by using Lenard-Jones 9-6 (L-J 9-6) potential with a cut-off distance of 12.5 Å combined with a long-range Columbic interaction. The combination rules for this L-J 9-6 potential were given by the equations 1-2.

$$r_{ij}^{o} = \left(\frac{(r_i^o)^6 + (r_j^o)^6}{2} \right)^{\frac{1}{6}} \quad (1)$$

$$\varepsilon_{ij}^{o} = \frac{\sqrt[2]{\varepsilon_i^o \varepsilon_j^o} \left(r_i^o r_j^o\right)^3}{(r_i^o)^6 + (r_j^o)^6} \quad (2)$$

The interfacial interactions are the critical factor that affects the structure of organic molecule on the surface as well as its rheological properties under confined conditions. As shown in Figure 1, the interaction between alkane and iron was derived from *ab initio* calculations, where the adsorption energy between C_2H_6 and iron surface was measured by Govender *et al.* [19].

Table 1. *Potential parameters of Buckingham potential for FeO and Fe_2O_3*

	$z(e)$	$B(eV)$	$\rho(A)$	$C(A^6eV)$
O	-0.945	9022.821	0.265	85.092
Fe^{2+}	0.945	13032.949	0.190	0.000
Fe^{3+}	1.4175	8020.285	0.190	0.000

Values for B, ρ and C corresponding to iron cation-oxygen and oxygen-oxygen interaction, the cation-cation interaction being described only by Columbic repulsive forces.

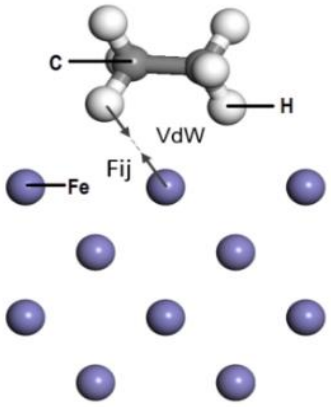

Figure 1. *The adsorption model of C_2H_6 adsorbate on Fe(100) surface reconstructed from reference [19]. The interaction between ethane and iron surface was described using Van der Wall interaction.*

JTE
HCMUTE
ISSN: 2615-9740

JOURNAL OF TECHNICAL EDUCATION SCIENCE
Ho Chi Minh City University of Technology and Education
Website: https://jte.hcmute.edu.vn/
Email: jte@hcmute.edu.vn

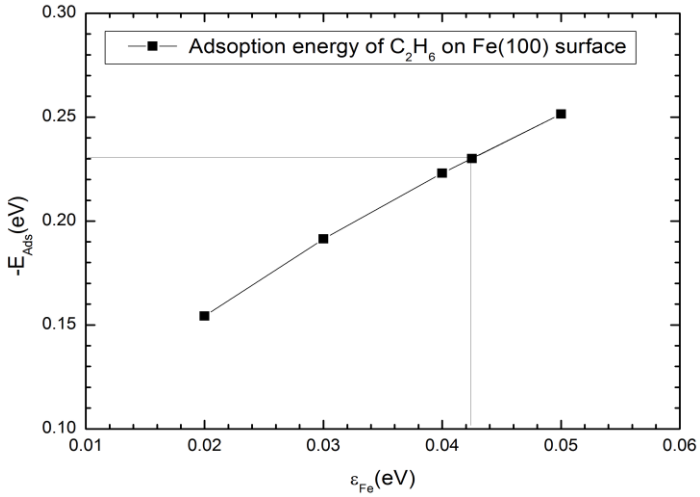

Figure 2. *Adsorption energy -E_{ads} of ethane C_2H_6 on Fe(001) surface as a function of well-depth energy of iron ε_{Fe}.*

The procedure to calibrate this interaction parameter was implemented using their work with L-J 9-6 potential. This parameterization was carried out at absolute zero temperature. The ethane molecule and two upper iron layers were relaxed while the rest was fixed. In order to get consistent adsorption energy with Govender's result, the well-depth energy of iron (ε_{Fe}) for L-J 9-6 interaction between surface and lubricant was kept in range between 0.02 and 0.05 eV. The dependence of adhesive strength between ethane and iron surface on ε_{Fe} is presented in Figure 2, which indicates that the value for ε_{Fe} of 0.0425 eV is appropriate to represent the adsorption energy of E_{ad} = -0.23 eV from previous ab-initio calculation [19]. The non-bond interaction parameters between iron oxide surfaces and hexadecane were conducted from the COMPASS FF and semi-ionic oxide model proposed by Zhao et al. [20] (Table 2). The molecular model was constructed with hexadecane layer allocated above Fe(100), FeO(100), and Fe_2O_3(001) surfaces. The system domain sizes $D_x \times D_y \times D_z$ were roughly 35 ×35 × 60 $Å^3$ in x, y, and z directions, respectively (Table 3). The thickness for each surface was roughly 10 Å and the initial thickness of fluid layer was 40 Å.

Table 2. *Non-bond Lenard-Jones potential parameters for interaction between iron/iron oxide surfaces and hexadecane.*

Atoms	Zhao's work [20]		Derived from COMPASS	
	$\varepsilon_0(eV)$	$r_0(Å)$	$\varepsilon_0(eV)$	$r_0(Å)$
O	0.0034	3.627	0.0097	3.627
Fe^{2+}	0.01858	3.950		3.950
Fe^{3+}	0.02149	4.077		4.077
	$\varepsilon_0(eV)$		$r_0(Å)$	
Fe	0.0425^a		2.6595	

Table 3. *Domain sizes and number of hexadecane molecules for each confined shear model*

Surfaces	$D_x(Å)$	$D_y(Å)$	$D_z(Å)$	No. of $C_{16}H_{34}$ molecules
Fe	34.40	34.40	60.00	94
FeO	34.98	34.98	60.00	94
Fe_2O_3(001)	34.88	35.25	60.00	94
Fe_2O_3(012)	32.50	40.28	60.00	94

JTE
HCMUTE
ISSN: 2615-9740

JOURNAL OF TECHNICAL EDUCATION SCIENCE
Ho Chi Minh City University of Technology and Education
Website: https://jte.hcmute.edu.vn/
Email: jte@hcmute.edu.vn

3. Results

Surface corrugation [21] – [25] and adhesive strength [23], [26] - [28] play a vital role on molecular structure of thin hydrocarbon film. Therefore, the influences of these factors were analysed. The obtained results in Table 4 shows that both COMPASS and Buckingham FF can predict the crystalline structure of different iron compounds. Regarding the solid material, the surface structure is different from its bulk due to the propensity of atomic rearrangement after cleaving the surface. Furthermore, the unrelaxed surfaces influence significantly the interaction energy of organic molecules on solid surfaces compared to the relaxed ones [5]. Therefore, the surfaces were relaxed to reduce the residual force and optimize the surface structure. In this relaxation, the bottom layers of the surfaces were constrained to reflect its bulk structure, while the others were unconstrained. As shown in Figure 3, a 2-nm-vacuum was added on the top of surfaces. A comparison between MD, DFT and experiments in Table 5 shows the changes in inter-atomic layer spacing of iron surface with the relaxations of the top atomic layer of 1.9% and 9.4% for EAM/FS and COMPASS, respectively. This table also shows that the relaxation obtained from EAM/FS is closer with DFT calculation and experiments than COMPASS FF.

Table 4. *Lattice parameters for iron and iron oxides obtained from EAM/FS [16] for Fe, Buckingham for FeO and Fe_2O_3 [29, 30], COMPASS, and experiments*

Compounds	Used FF in this work	COMPASS	Expt.
Fe	a = b = c = 2.866 Å α = β = γ = 90°	a = b = 2.534 Å c = 3.583 Å α = β = γ = 90°	a = b = c = 2.840 Å[a] α = β = γ = 90°[a]
FeO	a = b = c = 4.373 Å α = β = γ = 90°	a = b = c = 4.331 Å α = β = γ = 90°	a = b = c = 4.33 Å[b] α = β = γ = 90°[b]
Fe_2O_3	a = b = 5.048 Å c = 13.931 Å α = β = 90° γ = 120°	a = b = 5.055 Å c = 13.411 Å α = β = 90° γ = 120°	a = b = 5.035 Å[c] c = 13.747 Å[c] α = β = 90°[c] γ = 120°[c]

[a]Lattice parameters for iron obtained from experiment in Ref. [16]
[b]Experimental lattice parameters for FeO from Ref. [29]
[c]Experimental lattice parameters for Fe_2O_3 from Ref. [30]

Table 5. *The structure of Fe(100) surface containing the top five layers after relaxation*

Distances	Initial	COMPASS		EAM/FS		Ref.	
	d_0 (Å)	d (Å)	Δd (%)	d (Å)	Δd (%)	DFT [31] (%)	Expt. [32] (%)
$Fe^{[1]} - Fe^{[2]}$	1.433	1.569	9.4	1.461	1.9	-3.0	-1.4 ± 3
$Fe^{[2]} - Fe^{[3]}$	1.433	1.467	2.4	1.410	-1.6	1.7	5 ± 2
$Fe^{[3]} - Fe^{[4]}$	1.433	1.443	0.7	1.436	0.2		
$Fe^{[4]} - Fe^{[5]}$	1.433	1.437	0.3	1.432	-0.1		

The relaxation for FeO(100) surface using COMPASS potential is presented in Table 6 with the changes in z coordinate of the top layers are -2.2% for Fe and -8.6% for O, while there are -6.0% for Fe and 6.9% for O for Buckingham. The result indicated that the FeO(100) surface atoms were shrunk by using COMPASS FF, whereas they were expanded with Buckingham. The contraction tendency of COMPASS was consistent with that obtained by Wang *et al.*[33]. However, considering surface corrugation, the surface described by the Buckingham FF was smoother and more consistent with their DFT calculation. The inter-atomic space between Fe and O atoms on the top layer are $d_{Fe\text{-}O}$ = -0.9% for Buckingham potential, whereas this value is 6.4% for COMPASS. In general, there was a discrepancy of both COMPASS and Buckingham FF in comparison with DFT calculation in describing the surface structure of FeO(100), but the differences are rather small.

JTE
HCMUTE
ISSN: 2615-9740

JOURNAL OF TECHNICAL EDUCATION SCIENCE
Ho Chi Minh City University of Technology and Education
Website: https://jte.hcmute.edu.vn/
Email: jte@hcmute.edu.vn

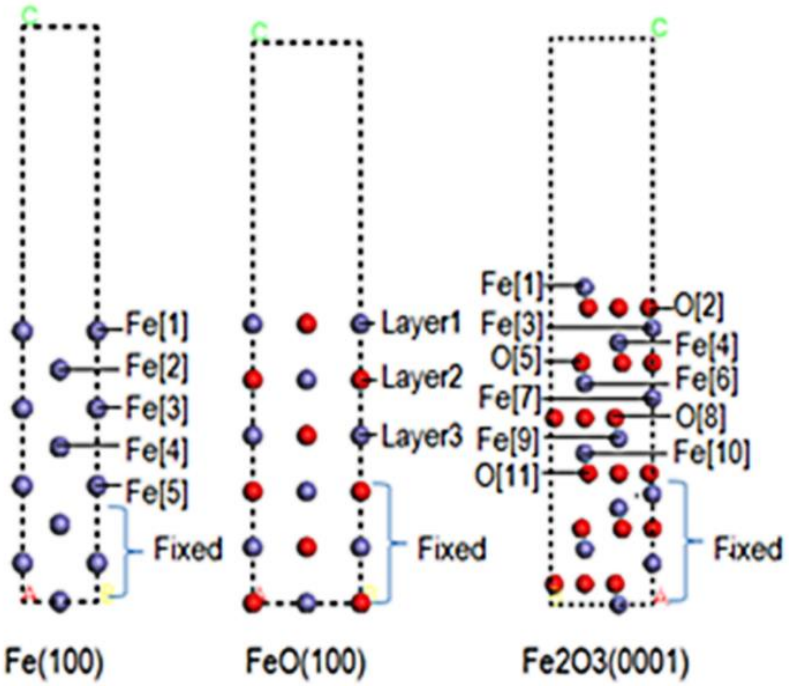

Figure 3. *Cross-sections of Fe(100), FeO(001), Fe_2O_3(0001) slabs used in calculation. The Fe and O atoms are purple and red, respectively. Lower layers are fixed while the others are free and a vacuum of 2nm is added on the top of the surfaces.*

Table 6. *The structure of $FeO(100)$ surface containing the top three layers after relaxation*

	COMPASS			Buckingham			DFT^a		
	Layer 1	Layer 2	Layer 3	Layer 1	Layer 2	Layer 3	Layer 1	Layer 2	Layer3
$\Delta z_{Fe}/\%$	-2.2	-2.6	-1.8	6.0	4.9	3.1	-2.7	-1.6	-1.2×10^{-6}
$\Delta z_O/\%$	-8.6	-3.0	-2.2	6.9	4.7	3.2	-3.2	-1.5	0.5×10^{-6}
	COMPASS			Buckingham			DFT^a		
	Δd_{12}	Δd_{23}	Layer 1	Δd_{12}	Δd_{23}	Layer 1	Δd_{12}	Δd_{23}	Layer1
$d_{Fe-O}/\%$	0.8	-0.5	6.4	1.3	1.7	-0.9	-6.2	-4.8	0.02
$d_{O-Fe}/\%$	-6.0	-1.2	-6.4	2.0	1.5	0.9	-7.8	-4.4	-0.02

[a]Result obtained from DFT calculation from Ref. [33]

For Fe_2O_3(001) surface, the inter-atomic spacing for the top surface layer moves inward 54%, whereas there is an expansion of 11.9% for the first sub-layer using Buckingham. This surface relaxation is consistent with the results obtained from DFT calculation (Table 7). In contrast, COMPASS predicts the respective contractions of 135.9% and 39.3% for the top and the first-sub surface layers, indicating that Buckingham FF is more accurate than COMPASS in describing the surface structure of Fe_2O_3.

JTE HCMUTE
ISSN: 2615-9740

JOURNAL OF TECHNICAL EDUCATION SCIENCE
Ho Chi Minh City University of Technology and Education
Website: https://jte.hcmute.edu.vn/
Email: jte@hcmute.edu.vn

Table 7. *Structure of $\alpha - Fe_2O_3(0001)$ surface containing six repeat units before and after relaxation. However, only the top three repeat units are shown.*

Distances	Initial	COMPASS		Buckingham		DFT		
	d_0 (Å)	d (Å)	Δd (%)	d (Å)	Δd (%)	Trainor Ref.[34] Δd(%)	Wang Ref.[35] Δd(%)	Chambers Ref.[36] Δd(%)
$Fe^{[1]} - O^{[2]}$	0.846	-0.335	-139.5	0.39	-54.0	-65	-57	-59
$O^{[2]} - Fe^{[3]}$	0.846	0.513	-39.3	0.946	11.9	7	7	17
$Fe^{[3]} - Fe^{[4]}$	0.595	0.556	-6.5	0.261	-56.2	-26	-33	-17
$Fe^{[4]} - O^{[5]}$	0.846	0.928	9.7	1.071	26.5	13	15	41
$O^{[5]} - Fe^{[6]}$	0.846	1.099	29.9	0.942	11.4	5	5	
$Fe^{[6]} - Fe^{[7]}$	0.595	0.306	-48.5	0.542	-8.9	-4	-3	
$Fe^{[7]} - O^{[8]}$	0.846	0.961	13.5	0.862	1.9	2	1	
$O^{[8]} - Fe^{[9]}$	0.846	0.826	-2.4	0.891	5.3	0	4	
$Fe^{[9]} - Fe^{[10]}$	0.595	0.681	14.5	0.567	-4.7			
$Fe^{[10]} - O^{[11]}$	0.846	0.749	-11.5	0.868	2.6			

The model to investigate hexadecane adsorbed onto iron and iron oxides surfaces was carried out. The modelling lubricant consisted of a 10-Å-thick hexadecane film constituted of 40 molecules and fully covered on a square surface with the width of 35 Å for each lateral dimension (Figure 4). This adsorption simulation was carried out with a NVT simulation at room temperature 300K. During the dynamic simulations, the hexadecane molecules tended to vibrate under thermostated condition and moved toward the solid surfaces due to their non-bond interactions with the lubricant. Consequently, as presented in Figure 5, the adsorption energies increase with the simulation time and become more stable after 100 ps. The average adsorption energy of hexadecane during the last 250 ps on iron surface was smaller than those gained from iron oxides. Particularly, the respective $-E_{ads}$ values of 18.5, 18.8, and 18.9 eV for Fe(100), FeO(100), and Fe_2O_3(001) surfaces. Regarding the iron oxides surfaces with interfacial interaction taken from the reference, the adsorption energy for $Fe_2O_3(0001)$ was surface 19.3 eV – slightly larger than FeO(100) (roughly 18.8 eV). Conversely, there was a significantly larger adsorption energy on the FeO(100) surface (around 21.9 eV) compared with the Fe_2O_3(001) surface (roughly 18.9 eV) when using the COMPASS FF (Figure 5).

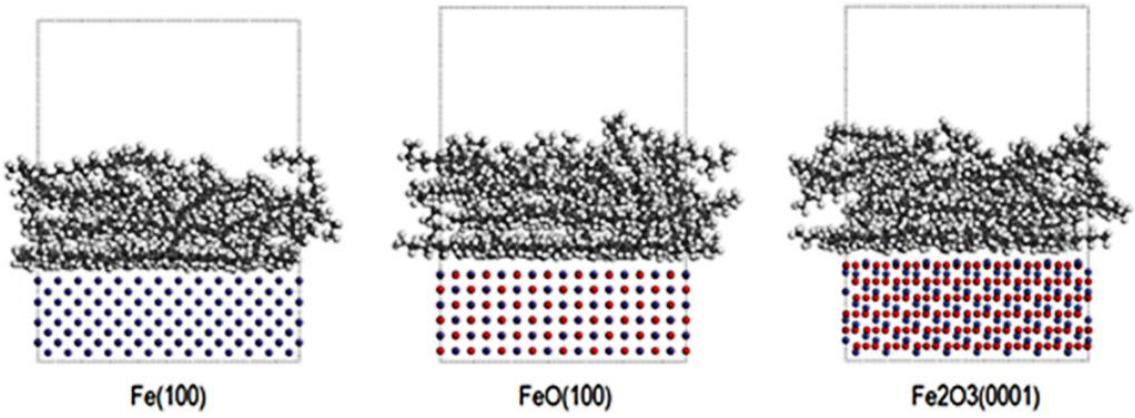

Figure 4. *Snapshot of thin hexadecane film adsorbed on Fe(100), FeO(100), and Fe_2O_3(001) 2D-periodic slabs at 0.5 ns. The system involves 40 hexadecane molecules adsorbed on a square surface area of a 35 Å for each side dimension and 10 Å for slab thickness.*

JTE
HCMUTE
ISSN: 2615-9740

JOURNAL OF TECHNICAL EDUCATION SCIENCE
Ho Chi Minh City University of Technology and Education
Website: https://jte.hcmute.edu.vn/
Email: jte@hcmute.edu.vn

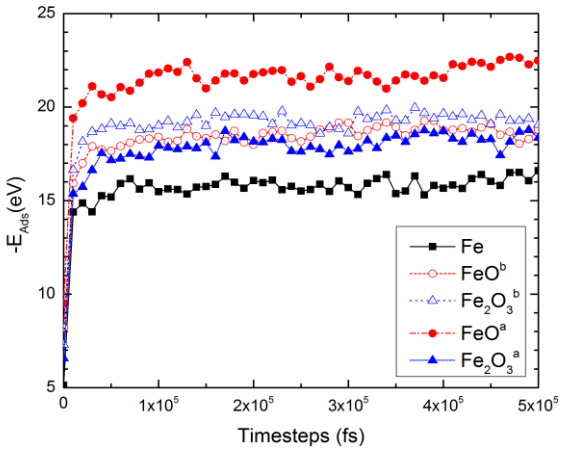

(i)

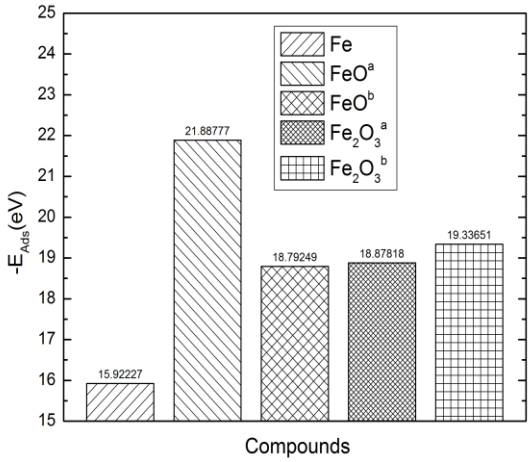

(ii)

Figure 5. *(i) Time evolution of adsorption energy (E_{ads}); and (ii) average E_{ads} values of fully covered hexadecane film on Fe(100), FeO(100), and Fe_2O_3(001) surfaces. ^{a,b} denote the model with interfacial interaction parameters obtained from COMPASS, and Buckingham FFs, respectively.*

An interesting feature is that although the adsorption energies are substantially different between two implemented solid-liquid interaction FFs for FeO(100) surface, the atomic concentration profiles of hexadecane back-bone in Figure 6a are similar. In contrast, there is a moderate difference of the peak of atomic density of the first hexadecane layer on Fe_2O_3(001) surface despite the obtained adsorption energies from both FFs are close (Figure 6b). The interpretation for this observation could be due to the fact that both COMPASS and Buckingham FFs can simulate properly the surface structure of FeO(100), whereas only Buckingham FF could predict accurately the surface properties of Fe_2O_3(001). The rearrangement of surface atoms is distinct for different FFs, which result in the discrepancies in ordering structure of hexadecane lubricant on Fe_2O_3(001) surface. The separation between the first hexadecane layer and the iron surface is 3.2 Å, while it is 3.5 Å for iron oxides. This value was consistent with that obtained from Li [5] and Claire [6]. In addition, the numbers of adsorbed back-bond carbon atoms in the first layer and the saturated carbon densities in Table 8 indicate a slight difference between chosen FFs, while there is a significant difference between the surfaces with the largest number of adsorbed carbon atoms found on

JTE
HCMUTE
ISSN: 2615-9740

JOURNAL OF TECHNICAL EDUCATION SCIENCE
Ho Chi Minh City University of Technology and Education
Website: https://jte.hcmute.edu.vn/
Email: jte@hcmute.edu.vn

FeO(100). Therefore, there is an effect of surface structure and applied FFs on the atomic density at solid-fluid interface.

Table 8. *Computed distance between the first nearest layer of hexadecane to the surface and to the second layer, the number of saturated carbon atoms and its density, the adsorption energy as well as its mean value for each CH_2 group. The model with interfacial interaction parameters were obtained from: [a]COMPASS, [b]Ref. [20]*

Surfaces	Distance (Å)		No. of C atoms on 1^{th} layer	Saturated density Atom ($\frac{Atom}{100\ Å^2}$)	Adsorption energy (eV)	Adsorption energy/CH_2 (eV)
	Surface -1^{th} layer	$1^{th}-2^{th}$ layer				
Fe	3.0	4.5	184	15.6	15.922	0.025
FeO^a	3.5	4.5	194	16.2	21.888	0.034
FeO^b	3.5	4.5	190	15.8	18.792	0.029
$Fe_2O_3^a$	3.5	4.5	192	15.6	18.878	0.029
$Fe_2O_3^b$	3.3	4.5	185	15.0	19.337	0.030

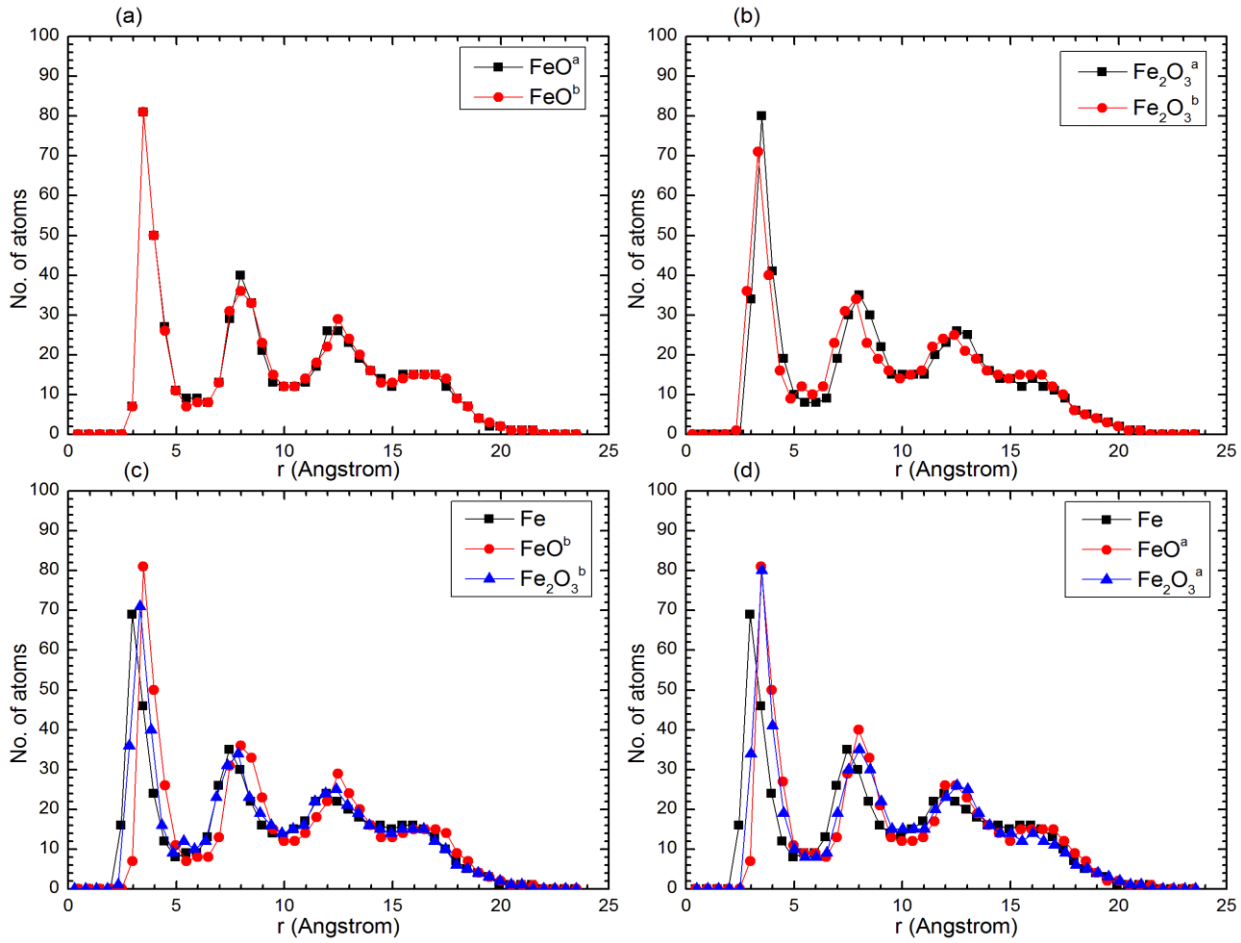

Figure 6. *Atomic density profiles across the film thickness of hexadecane in normal direction of: (a) FeO surfaces; (b) Fe_2O_3 surfaces; (c), (d) Fe, FeO, and Fe_2O_3 surfaces. The model with interfacial interaction parameters were obtained from: [a]COMPASS FF, [b]Ref. [20]*

4. Conclusions

The molecular dynamic simulation had been carried out to analyse the effects of iron and its binary oxides surface to the adsorption of hexadecane on these surfaces. By employing a reliable force field for lubricant molecules, the obtained results showed a good prediction of bulk hexadecane adsorption ability. Regarding the behaviour of hexadecane on iron and iron oxide surfaces, MD results provided that it preferred to adsorb on iron oxide surface rather than its pure metal one, and layer forming was observed in these cases.

REFERENCES

[1] S.L. Tait et al., "n-alkanes on Pt(111) and on C(0001)/Pt(111): Chain length dependence of kinetic desorption parameters," *J. Chem. Phys.*, vol.125, 234308, 2006.
[2] R.M. Slayton et al., Desorption Kinetics and Adlayer Sticking Model of n-Butane, n-Hexane, and n-Octane on Al_2O_3(0001), J. Phys. Chem. 99, pp 2151-2154, 1995.
[3] S.M. Wetterer et al., "Energetics and Kinetics of the Physisorption of Hydrocarbons on Au(111)," *J. Phys. Chem. B*, vol.102, pp.9266-9275, 1998.
[4] M.A. San-miguel and P.M. Rodger, "Simulation of Deposition of Wax to Iron Oxide Surfaces," *Mol. Simul.*, vol.26, pp.193-216, 2001.
[5] C. Li, P. Choi, "Molecular Dynamics Study of the Adsorption Behavior of Normal Alkanes on a Relaxed α-Al_2O_3 (0001) Surface," *J. Phys. Chem. C*, vol.111, pp.1747-1753, 2007.
[6] P. de Sainte Claire et al., "Simulations of hydrocarbon adsorption and subsequent water penetration on an aluminum oxide surface," *J. Chem. Phys.*, Vol.106, pp.7331, 1997.
[7] K. Bolton et al., "Comparison of Explicit and United Atom Models for Alkane Chains Physisorbed on α-Al_2O_3 (0001)," *J. Phys. Chem. B*, vol.103, pp.3885-3895, 1999.
[8] R.Z. Lei, A.J. Gellman and B.E. Koel, "Desorption energies of linear and cyclic alkanes on surfaces: anomalous scaling with length," *Surf Sci.*, vol. 554, pp. 125-140, 2004.
[9] S.L. Tait et al., "n-alkanes on MgO(100). II. Chain length dependence of kinetic desorption parameters for small n-alkanes," *The Journal of Chemical Physics*, vol.122, 2005.
[10] K.R. Paserba and A.J. Gellman, "Effects of conformational isomerism on the desorption kinetics of n-alkanes from graphite," *The Journal of Chemical Physics*, vol.115, pp.6737-6751, 2001.
[11] A.B. Anderson, "Interaction of hydrogen, carbon, ethylene, acetylene, and alkyl fragments with iron surfaces. Catalytic hydrogenation, dehydrogenation, carbon bond breakage, and hydrogen mobility," *JACS*, vol.99, pp.696-707, 1977.
[12] M.B. Lee et al., "Activated dissociative chemisorption of CH_4 on Ni(111): Observation of a methyl radical and implication for the pressure gap in catalysis," *The Journal of Chemical Physics*, vol.85, pp.1693-1694, 1986.
[13] A.V. Hamza and R.J. Madix, "The activation of alkanes on Ni(100)," *Surf Sci.*, vol.179, pp.25-46, 1987.
[14] P.D. Szuromi et al., "Adsorption and reaction of n-alkanes on the platinum (110)-(1 .times. 2) surface," *The Journal of Physical Chemistry*, vol.89, pp.2497-2502, 1985.
[15] H. Sun, "COMPASS: An ab Initio Force-Field Optimized for Condensed-Phase Applications Overview with Details on Alkane and Benzene Compounds," *J. Phys. Chem. B*, vol.102, pp.7338-7364, 1998.
[16] M.I. Mendelev et al., "Development of new interatomic potentials appropriate for crystalline and liquid iron," *Philos. Mag.*, vol.83, pp.3977-3994, 2003.
[17] B. Guillot, N. Sator, "A computer simulation study of natural silicate melts. Part I: Low pressure properties," *Geochim. Cosmochim. Acta*, vol.71, pp. 1249-1265, 2007.
[18] B. Guillot, N. Sator, "A computer simulation study of natural silicate melts. Part II: High pressure properties," *Geochim. Cosmochim. Acta*, vol.71, pp. 4538-4556, 2007.
[19] A. Govender et al., "First-Principles Elucidation of the Surface Chemistry of the C_2H_x (x = 0–6) Adsorbate Series on Fe(100)," *Molecules*, vol.18, pp.3806-3824, 2013.
[20] L. Zhao et al., "Semi-ionic Model for Metal Oxides and Their Interfaces with Organic Molecules," *J. Phys. Chem. C*, vol.111, pp.10610-10617, 2007.
[21] T. Ohara and D. Torii, "Molecular dynamics study of thermal phenomena in an ultrathin liquid film sheared between solid surfaces: The influence of the crystal plane on energy and momentum transfer at solid-liquid interfaces," *J. Chem. Phys.*, vol.122, pp. 214717, 2005.
[22] A. Jabbarzadeh et al., "The structural origin of the complex rheology in thin dodecane films: Three routes to low friction," *Tribol. Int.*, vol.40, pp 1574-1586, 2007.
[23] H. Berro et al., "Molecular dynamics simulation of surface energy and ZDDP effects on friction in nano-scale lubricated contacts," *Tribol. Int.*, vol.43, pp.1811-1822, 2010.
[24] D. Savio et al., "A Model for Wall Slip Prediction of Confined n-Alkanes: Effect of Wall-Fluid Interaction Versus Fluid Resistance," *Tribol. Lett.*, vol.46, pp. 11-22, 2012.
[25] V. Kalyanasundaram et al., "Molecular Dynamics Simulation of Nanoconfinement Induced Organization ofn-Decane," *Langmuir*, vol.25, pp. 7553-7560, 2009.
[26] E. Manias et al., "Stick and Slip Behaviour of Confined Oligomer Melts under Shear. A Molecular-Dynamics," *Study EPL (Europhysics Letters)*, vol.24, pp. 99-104, 1993.
[27] S.T. Cui et al., "Molecular simulation of the transition from liquidlike to solidlike behavior in complex fluids confined to nanoscale gaps," *The Journal of Chemical Physics*, vol.114, pp. 7189, 2001.
[28] I.G. Wood et al., "Thermoelastic properties of magnesiowustite, (Mg_1-xFe_x)O: determination of the Anderson-Gruneisen parameter by time-of-flight neutron powder diffraction at simultaneous high pressures and temperatures," *J. Appl. Crystallogr.*, vol.41, pp. 886-896, 2008.
[29] H. Fjellvåg et al., "On the Crystallographic and Magnetic Structures of Nearly Stoichiometric Iron Monoxide," *J. Solid State Chem.*, vol.124, pp. 52-57, 1996.

[30] L.W. Finger and R.M. Hazen, "Crystal structure and isothermal compression of Fe_2O_3, Cr_2O_3, and V_2O_3 to 50 kbars," *J. Appl. Phys.*, vol.51, pp. 5362-5367, 1980.
[31] M. Altarawneh and S.A. Saraireh, "Theoretical insight into chlorine adsorption on the Fe(100) surface," *Phys. Chem. Chem. Phys.*, vol.16, pp.8575 - 8581, 2014.
[32] K. Legg et al., "Early stages of oxidation of the Fe{001} surface: Atomic structure of the first monolayer," *Phys. Rev. B*, vol.16, pp. 5271-5276, 1977.
[33] L. Wang and W. Chen, "Density functional theory for adsorption of HCHO on the FeO(100) surface," *Journal of Natural Gas Chemistry*, vol.19, pp. 21-24, 2010.
[34] T.P. Trainor et al., "Structure and reactivity of the hydrated hematite (0001) surface," *Surf Sci.*, vol.573, pp. 204-224, 2004.
[35] X.-G.W. Wang et al., "The Hematite (a-Fe_2O_3) (0001) Surface- Evidence for Domains of Distinct Chemistry," *Phys. Rev. Lett.*, vol.81, pp.1038-1041, 1998.
[36] S.A. Chambers and S.I. Yi, "Fe termination for α-Fe_2O_3(0001) as grown by oxygen-plasma-assisted molecular beam epitaxy," *Surf Sci.*, vol.439, pp. L785-L791, 1999.

Ta Dinh Hien currently works at Ho Chi Minh City University of Technology and Education, Vietnam. He received his bachelor, master, and Ph.D degrees in physics from Volgograd State Technical University, Russia, in 2009, 2011, and 2014, respectively. His research areas cover quantum physics and molecular dynamics simulations of solids and 2D materials.